

# Investigating Deviations from Dynamical Randomness with Scaling Indices

HARALD ATMANSPACHER

*Institut für Grenzgebiete der Psychologie  
Wilhelmstrasse 3a, D-79098 Freiburg, Germany  
and  
Max-Planck-Institut für extraterrestrische Physik  
Giessenbachstrasse, D-85740 Garching, Germany*

HERBERT SCHEINGRABER

*Max-Planck-Institut für extraterrestrische Physik  
Giessenbachstrasse, D-85740 Garching, Germany*

**Abstract**—The information contained in any given experimental time series can be utilized more exhaustively when *transition* probabilities between states rather than state probabilities alone are studied. Using advanced techniques of time series analysis, it is shown that deviations from *dynamical* randomness indicate evidence for unexpected *temporal* correlation features in selected data sets taken from a mind-matter experiment conducted at Freiburg (Germany). The techniques of analysis and a proper error estimation are briefly described, and some preliminary first results are presented. They encourage further inquiry into *processual* aspects of deviations from randomness in addition to more straightforward analyses of state probabilities.

**Keywords:** transition probabilities — scaling indices — deviations from randomness — temporal correlations in mind-matter data.

## 1. Introduction

Among other problem areas in the general framework of mind-matter research there is the basic question as to whether there are presently unknown relationships between physical systems and mental activities of human agents. Avoiding any speculations with respect to specific concepts of correlations, interactions, and causal or other influences between physical systems and mental systems, the mere formulation of this question presupposes a minimal methodological (not ontological) dualism of mind and matter without which it could not even be phrased. It has to be specified in order to lead to researchable problems. The special type of question addressed here is whether the randomness of a physically random system changes when human agents are asked to carry out certain “intentional tasks” that are defined so as to correspond to deviations from randomness in the behavior of the system.

Randomness is itself a concept that needs to be considered in more detail. First, there is the much discussed question of whether randomness or chance is

an “ontic” property of the material world, without any reference to the knowledge of observers, or whether it is an “epistemic” expression of our limited knowledge about an ontic world. Another most obvious problem with which any working scientist is familiar arises from the fact that for empirical purposes the mathematical, measure theoretic definition of probability a la Kolmogorov has to be backed up by an interpretation in terms of a limit of infinitely many independent realizations of an event. In practice, this is impossible to achieve. We always deal with finitely many events, they are never identical in every respect, and it has to be checked carefully whether and in what sense they are really independent of each other.

The finiteness of any empirical collective of events has the consequence that many mathematical theorems about probabilities (based on the limit  $N \rightarrow \infty$ ) must be applied with caution. For instance, in the area of complex systems research, many examples are known for which limit theorems (*e.g.*, laws of large numbers) are not naively applicable and ergodicity must not be implicitly presupposed. Novel approaches and techniques of modern statistics such as second order statistics or large deviations statistics (Atmanspacher, R ath, and Wiedenmann, 1997) offer new insights beyond a standard characterization of a distribution in terms of its first two moments. For appropriate methods of analyzing finite collectives in such situations, it has been proven necessary to characterize the concept of randomness with reference to the range of  $N$  with which one is empirically dealing.

Another important topic is the independence of events as members of a random collective. It is well known that distributions of states of a system can be perfectly random in the sense that they are perfectly represented, *e.g.*, by a Gaussian distribution, but nevertheless there can be non-random features, *e.g.*, correlations, as far as the transition probabilities between states (*i.e.*, the dynamics of the system) are concerned. In such a case, individual events are not independent. They depend on their prehistory and show significant temporal correlations. Correlations are significant if they deviate (at a level to be specified) from the amount of correlations expected due to the finiteness of the random collective. A number of measures that characterize and distinguish these different kinds of randomness have been analyzed and compared with each other by Wackerbauer *et al.* (1994). For an extensive study addressing dynamical randomness due to different kinds of stochastic processes see Gaspard and Wang (1993).

In Section 2 we give some basic arguments as to why dynamical aspects of randomness are important. Section 3 introduces a method of time series analysis capable of detecting deviations from (dynamical or non-dynamical) randomness with high sensitivity. This method is applied to data from an experiment described in Section 4.1. In Section 4.2 we sketch some details about proper error estimates for the analysis, and Section 4.3 discusses some first results from a small set of data involving human agent intention. Section 4 is a condensed version of a more comprehensive presentation in Atmanspacher *et al.* (1999). Section 5 concludes the paper with some perspectives.

## 2. Why Transition Probabilities?

Let us consider a state space  $A$  with a (homogeneous or non-homogeneous) partition  $P = \{A_i\}_{i=1}^N$  such that  $\bigcup A_i = A$  and  $A_i \cap A_j = \emptyset \forall i \neq j$ . If we assume that states  $\omega$  of a system can be represented as points in  $A$  then each state  $\omega$  can be assigned to a cell  $A_i$  of the partition. Given an overall probability measure  $\mu$  on  $A$ , the probability to find the state  $\omega$  in cell  $A_i$ , briefly denoted *state probability*, is

$$p_i = \mu(A_i). \quad (1)$$

Since the state is assumed to be somewhere in  $A$ , the state probabilities are normalized,

$$\sum_{i=1}^N p_i = 1. \quad (2)$$

Supposing that the states  $\omega$  are not stationary but evolve dynamically in  $A$ , each  $\omega$  has a predecessor and a successor. Let  $p_{ij}$  be the joint probability that the sequence  $\omega \in A_i \rightarrow \omega \in A_j$  occurs in any two successive steps in the dynamics, for instance described by a stochastic process (for more details see Doob, 1953). Then

$$p_{i \rightarrow j} = \frac{p_{ij}}{p_i} = \begin{pmatrix} p_{1 \rightarrow 1} & \cdots & p_{1 \rightarrow N} \\ \cdots & \cdots & \cdots \\ p_{N \rightarrow 1} & \cdots & p_{N \rightarrow N} \end{pmatrix} \quad (3)$$

is the conditional probability that, given  $\omega \in A_i$ , the successor of  $\omega$  is  $\omega' \in A_j$ . The matrix in Equation (3) is called a transition matrix, its entries being the *transition probabilities*. Since each state has to be somewhere in the subsequent step, the transition probabilities have to be normalized in each row of the matrix,

$$\sum_{j=1}^N p_{i \rightarrow j} = 1. \quad (4)$$

In another terminology,  $p_{i \rightarrow j}$  is a forward transition probability, designed for purposes of predicting a future state given the present. One can similarly define backward transition probabilities, designed for purposes of retrodicting a past state given the present, by  $p_{i \leftarrow j} = p_{ij}/p_j$ . This would be the conditional probability that, given  $\omega \in A_j$ , the predecessor of  $\omega$  is  $\omega' \in A_i$ . In general,  $p_{i \rightarrow j} \neq p_{i \leftarrow j}$ .

After these definitions, it is easy to answer the question formulated in the title of the present section. *Stochastic processes with different transition matrices  $p_{i \rightarrow j}$  can produce the same state distribution  $p_i$ .* This is to say that

information about the transition matrix can help to distinguish between different processes generating the same state distribution. If there are reasons to believe that (almost) identical state distributions are generated by different processes, then, in order to distinguish them, one has to look for differences in the transition probabilities.

To discuss some straightforward examples, we consider two classes of stochastic processes, namely uniformly and doubly stochastic processes.

- *Uniformly* stochastic processes are characterized by an equidistribution of states,

$$p_i = 1/N \quad \forall i. \quad (5)$$

- *Doubly* stochastic processes are characterized by the fact that transition probabilities in *both* rows and columns are normalized,

$$\sum_{j=1}^N p_{i \rightarrow j} = \sum_{i=1}^N p_{i \rightarrow j} = 1 \quad \forall i, j. \quad (6)$$

Each doubly stochastic process is uniformly stochastic, but not *vice versa* (Feller, 1950, p. 399). For instance, a transition matrix of the form

$$p_{i \rightarrow j} = \begin{pmatrix} 1/N & \cdots & 1/N \\ \cdots & \cdots & \cdots \\ 1/N & \cdots & 1/N \end{pmatrix} \quad (7)$$

implies that  $p_i = 1/N \forall i$ , hence uniform stochasticity. Well-known examples are the fair coin ( $N = 2$ ) or the fair dice ( $N = 6$ ). Other examples for which the partition is usually much more refined are “fully developed chaos” in the logistic map (at  $r = 4$ ), or any white noise process, *i.e.*, processes of Markov order zero with no temporal correlations.

Not quite so simple are doubly stochastic processes with transition matrices satisfying Equation (6) with different entries. For example, a process with

$$p_{i \rightarrow j} = \begin{bmatrix} 1/3 & 2/3 \\ 2/3 & 1/3 \end{bmatrix} \quad (8)$$

also implies uniform stochasticity with  $p_i = 1/2$  for both states. More involved examples for this kind of doubly stochastic behavior are given by colored noise processes, *i.e.*, higher order Markov processes with temporal corre-

lations. Doubly stochastic processes include the special case of strictly deterministic (*e.g.*, periodic) processes. If

$$\sum_{i=1}^N p_{i \rightarrow j} \neq 1 \quad \forall i, j, \quad (9)$$

the corresponding stochastic process is not doubly stochastic. This is the general case, and it is easy to imagine that in this case identical state distributions can be generated by processes with totally different transition matrices. Some well-studied examples are the golden mean process, the even process, or the Misiurewicz process. For more details, see Young and Crutchfield (1994).

### 3. Scaling Indices

There are a number of standard techniques of time series analysis which have originally been developed for the analysis of linear systems. Tools such as autocorrelation functions and power spectra have been widely used in many fields of application. Particularly due to more recent interest in the non-linear dynamics of complex systems, there is a considerable amount of literature on non-linear time series (see, *e.g.*, Priestley, 1988; Tong, 1990; Kantz and Schreiber, 1997); for applications see additionally Deco, Schittenkopf and Schürmann (1997), Kanz, Kurths and Meyer-Kress (1998) and Schreiber (1999). A particularly illuminating example for the power of advanced time series techniques, enabling the detection of *phase* correlations in non-linear systems, has been reported by Rosenblum, Pikovsky and Kurths (1996). Among general topics such as optimal prediction, noise reduction, tests for stationarity and linearity, it is one of the central problems for many applications to distinguish between random and non-random contributions in a given time series. An extremely sensitive technique in this regard is the *scaling index analysis*, a procedure strongly inspired by the concept of multifractals (Mandelbrot, 1974; Halsey *et al.*, 1986).

Scaling indices essentially represent a fairly sophisticated and compact measure of correlations between data points (Paladin and Vulpiani, 1987). For a given point set they describe how the local density of the set around each point changes with increasing distance from that point. A convenient way to visualize this is in terms of a histogram  $N(\alpha)$  showing the number  $N$  of points in the set as a function of the scaling index  $\alpha$ . The scaling index  $\alpha$  (sometimes also denoted “crowding index”; Grassberger, Badii and Politi, 1988) is defined by

$$\alpha_i = \frac{\log n_i(\epsilon_2) - \log n_i(\epsilon_1)}{\log \epsilon_2 - \log \epsilon_1}, \quad (10)$$

where  $n_i(\epsilon)$  is the number of points within a box of size  $\epsilon$ , to be considered

around point  $i$  of the entire point set ( $i = 1, 2, \dots, N_{\text{tot}}$ ), and  $\epsilon_1 < \epsilon_2$ . The scaling index is thus defined for a specific range of  $\epsilon$ , which in turn defines a locality criterion with respect to which correlations are characterized by  $\alpha_i$ . Counting those boxes (to be constructed around points) that give rise to  $\alpha_i$ , a histogram  $N(\alpha)$  is obtained. For more details and additional references, see Atmanspacher, Scheingraber and Wiedenmann (1989) and Atmanspacher *et al.*, (1999).

For perfectly random distributions in a  $d$ -dimensional space, the ideal  $N(\alpha)$  histogram for infinitely many points is a  $\delta$ -function at  $\alpha = d$ . Due to the restrictions imposed by a finite number of points, non-zero  $\epsilon$ , and finite binning of  $\alpha$ ,  $N(\alpha)$  is broader and its mean is shifted toward values of  $\alpha$  smaller than  $d$ . The same happens for regular patterns with topological dimension  $n < d$ , where the ideal  $N(\alpha)$  for infinitely many points is a  $\delta$ -function at  $\alpha = n$ . It is intuitively clear that a scaling index analysis can be useful to discriminate between non-random features with  $n < d$  and a random background. For examples in various scientific areas see Atmanspacher, Scheingraber and Wiedenmann (1989), Morfill, Demmel and Schmidt (1994), Atmanspacher, Wiedenmann and Amann (1995), R ath and Morfill (1997), Wiedenmann, Scheingraber and Voges (1997), and Atmanspacher *et al.* (1999).

For faint non-random contributions dominated by a random distribution such a task is difficult since — depending on their nature — they typically appear as small deviations in the left wing of an  $N(\alpha)$  histogram characterizing randomness. For such situations, it is crucial to take care in selecting a good locality criterion (range of  $\epsilon$  over which  $\alpha_i$  is calculated) and in estimating errors in an appropriate manner.

If a correlation analysis based on a scaling index analysis is to be carried out for a time series (temporal sequence of data) rather than a spatial pattern, then it is necessary to represent the time series in a space with dimension greater than one. A standard way to achieve such a representation has been proposed by Packard *et al.* (1980) in order to reconstruct attractors of dissipative dynamical systems and extract their invariants. Our goal in the present study is less ambitious since we do not look for invariants of a real physical process but simply for correlations in the temporal sequence of data points in a time series.

Inspired by the delay coordinate technique of Packard *et al.*, we use the original time series  $\phi(t)$  to construct a number  $(d - 1)$  of additional time series, each delayed by a temporal interval  $\Delta t$  with respect to its predecessor. In this way, new coordinates  $x_i$  are obtained according to

$$\begin{aligned} x_1(t) &= \phi(t), \\ x_2(t) &= \phi(t + \Delta t), \\ &\vdots = \vdots \\ x_d(t) &= \phi(t + (d - 1)\Delta t) \end{aligned} \tag{11}$$

with

$$\vec{x}(t) = (x_1(t), x_2(t), \dots, x_d(t)). \quad (12)$$

In this manner, the original (one-dimensional) time series can be represented in a  $d$ -dimensional space, and the corresponding histogram  $N(\alpha)$  can be calculated. This allows us to discriminate regular (deterministic) contributions from random noise in the behavior of dynamical systems. In particular, non-random features in the transition probabilities (*i.e.*, correlations) between individual members of the time series can be detected in addition to non-random state probabilities. Such a task is fairly straightforward in the case of low-dimensional attractors (fixed points, limit cycles); compare, *e.g.*, Siffling (1996).

For investigations of less prominent non-random temporal features in a random background process, the analysis becomes more sophisticated. In this case, one would ideally proceed to embedding dimensions  $d$  as high as possible since the  $\alpha$ -range of  $N(\alpha)$  characterizing random contributions increases with  $d$  whereas the  $\alpha$ -range of the non-random part of  $N(\alpha)$  drops back with increasing  $d$ . This means that faint non-random contributions appearing as deviations in the left wing of the dominating random part of  $N(\alpha)$  become more pronounced and thus can be better discriminated as  $d$  is increased.

However, severe restrictions on the size of  $d$  are imposed by the length of the original time series. For as few as 1000 data points per time series, the point distribution resulting from the delay technique in  $d = 4$  is not dense enough to admit a statistically reasonable analysis. For 10,000 data points,  $d = 4$  is a reasonable upper limit for  $d$ . In addition, it is mandatory to carry out a proper error estimate since the  $N(\alpha)$  histogram for a random distribution of not more than 10,000 points deviates significantly from its limit for infinitely many points. Non-vanishing correlations are to be expected for random time series of finite length. The question is whether the scaling histogram of an empirically observed time series of finite length differs significantly from the expected histogram for a random time series with the same finite length. It makes absolutely no sense to compare empirically obtained  $N(\alpha)$  histograms for finite time series with  $N(\alpha)$  histograms as they are theoretically expected in the limit of infinitely long time series.

Significant deviations from a random distribution of points as detected by a scaling index analysis of a time series embedded in a  $d$ -dimensional space can have different origins. In particular, such deviations are not necessarily due to deviations from dynamical randomness, *i.e.*, temporal correlations in the time series. Moreover, the delay technique generating the embedding space can lead to delicate superpositions of different kinds of correlations that are difficult to separate from each other. It is therefore inevitable to apply additional procedures if one wants to disentangle genuinely temporal correlations from others; this issue will be taken up later on.

## 4. Data Analysis

### 4.1 Experimental

The prototype of the experimental setup from which data are taken for analysis goes back to Schmidt (1970). It has been refined and applied to a large range of empirical questions in the work of the Princeton Engineering Anomalies Research (PEAR) project within the last two decades. The general question behind that work is whether some “intentional activity” of human agents changes the output of physical systems which are expected to produce random events. The work of PEAR suggests that there are significant deviations from randomness when human agent intention is involved (Jahn *et al.*, 1997; see also Utts, 1991). A replication of the PEAR studies has been started at the Institut für Grenzgebiete der Psychologie und Psychohygiene (IGPP) at Freiburg in 1996. The present investigations refer to a small subset of data obtained in the IGPP replication study.

The material core of the experiment is a random event generator (REG) whose output (after some processing) consists of binary sequences. In the IGPP replication study, a portable random event generator, different from the REG originally developed and used by PEAR, was utilized. More details concerning these two sources of randomness can be found in Nelson, Bradish and Dobyms (1989) and Bradish (1993). Both sources are semiconducting devices, producing a mixture of quantum and thermal noise. After 200 bits (0s and 1s) were generated by the REG, the number of 1s is counted and the result is taken as the outcome of a single “trial” for the experiment.

Sequences of 100 and 1000 trials, respectively, constitute experimental “runs” consisting of successive integer “raw data”  $x_i$  scattered around a mean value of 100 with a standard error of  $\sqrt{50}$ . The trials of a run can be graphically represented (depending on feedback options) on a monitor. This representation  $\xi_i$  is obtained from the raw data  $x_i$  by

$$\xi_i = \sum_{j=1}^i x_j - 100i \quad (13)$$

or, recursively, by

$$\begin{aligned} \xi_1 &= x_1 - 100, \\ \xi_i &= \xi_{i-1} + (x_i - 100) \quad \text{for } i > 1, \end{aligned} \quad (14)$$

The series  $\xi_i$  is thus cumulative in the sense that a constant value above (below) 100 in the raw data would produce a monotonically increasing (decreasing) graph for  $\xi_i$  on the monitor. If the REG produces random numbers,

the overall expectation (for  $N \rightarrow \infty$ ) is that the curve  $\xi_i$  does not significantly deviate from the baseline 0.

According to the experimental protocol, human agents are asked to intentionally try to cause the curve to rise above or fall below the baseline, or to be intentionally neutral with respect to the appearance of the curve in different runs. (They are *not* explicitly asked to achieve deviations from randomness.) The corresponding “modes of intention” are denoted as “high,” “low,” and “baseline.” It is left to the agents how to realize each of these modes of intention cognitively. The particular intention per run is preselected randomly or by the agents themselves.

An experimental “session” consists of 1000 trials per each intention. For runs consisting of 100 (1000) trials, a session therefore amounts to 10 runs (1 run) per intention, *i.e.*, 30 (3) runs in total. For the analysis described below, data from agents with 10 sessions each have been used, *i.e.*, 10,000 trials per agent and intention. To avoid artificial correlation effects, the analysis has been based on the raw data  $x_i$  rather than the cumulative data  $\xi_i$ . Regarding the values assumed by  $x_i$  (roughly between 70 and 130) as states, the histogram of those states represents a state distribution.

The most prominent result obtained from analyses of the data pool collected by PEAR is that the mean value of the distribution of state probabilities (integer values  $x_i$ ) shows small systematic shifts above and below the expected mean of 100.0 for experimental conditions with high and low intention, respectively. The precise values as given by Table 1 in Jahn *et al.* (1997) are 100.026 for high, 99.984 for low, and 100.013 for baseline. Although the corresponding high–low separation of 0.042 is tiny, Jahn *et al.* (1997) report an overall  $z$ -score of 3.81 (with  $p \approx 7 \times 10^{-5}$ ) for the entire set of individual sessions. (For more details on the importance of  $z$ -scores and effect sizes in this and related studies see Utts (1991) and Delaney (1996)).

This is not the only result that was found by PEAR. After perusing the available literature, it appears that the analyses that have been done are all based on state probabilities and do not explicitly take transition probabilities into account. As shown in Section 2, it is interesting to focus on those transition probabilities between states since they can reveal information that is not available in the distribution of state probabilities alone.

In the following, we describe a scaling index analysis of time series obtained from a physical random event generator (REG) as described above under two different conditions: 1. The output of the REG is sampled without any additional constraints on the experimental setup; the corresponding data are used for calibration and allow us to derive a reasonable error estimate; 2. The output of the REG is analyzed for situations in which human agents are asked to carry out “intentional tasks” that are defined so as to correspond to non-random contributions to the activity of the REG.

The main conceptual difference between the scaling index analysis and the analyses carried out by PEAR so far consists of the fact that we do explicitly

address transition probabilities between states together with state probabilities. (Of course, there are other possibilities to realize such a purpose; see, *e.g.*, Kurths *et al.*, 1995.) As mentioned above, the data used for this purpose are data from the IGPP replication study. This study is not yet finished, implying that any assignment of individual runs to agent intentions is kept hidden so far. Therefore, our analysis is strictly bound to an analysis of deviations from randomness and does not refer to specific agent intentions.

#### 4.2 Errors

In experiments such as those briefly sketched in Section 4.1, one should by no means expect easily detectable, major deviations from a perfectly random distribution. For this reason, extremely careful error estimates are mandatory for a sound scaling index analysis. These error estimates have to be based on the same parameters as used in the analysis of those data taken under the influence of human agents. For time series consisting of 10,000 data points  $\Delta t = 1$  and  $d = 4$  have been selected. Scaling indices  $\alpha$  are binned in steps of 0.01.

For an optimal locality criterion,  $\epsilon_1 = 4.6$  and  $\epsilon_2 = 12.7$  have been determined by minimizing the differences between  $N(\alpha)$  histograms for calibration data (Atmanspacher *et al.*, 1999). This means that we look for correlations on the mentioned distance scale only. Correlations on larger scales, *e.g.*, approaching the diameter of the point distribution as a whole, are left out of consideration. Calibration data are taken from the experimental random number device as described in Section 2. Figure 1 shows an example of a resulting  $N(\alpha)$  histogram.

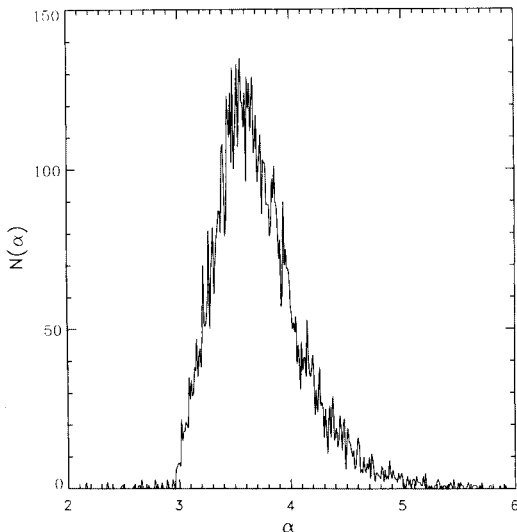


Fig. 1. Histogram of scaling indices  $N(\alpha)$  for a set of 10,000 calibration data obtained from the IGPP replication of the PEAR experiment. The embedding dimension is  $d=4$  so that the theoretical expectation for  $N \rightarrow \infty$  (and  $\Delta\alpha \rightarrow 0$ ) is a  $\delta$ -function at  $\alpha=4$ .

The relative differences (normalized with respect to the total number  $N_{\text{tot}}$  of points)

$$\delta_{1,2}(\alpha) = \frac{1}{N_{\text{tot}}} (N(\alpha)_1 - N(\alpha)_2) \quad (15)$$

between any two histograms  $N(\alpha)_1$  and  $N(\alpha)_2$  (for specifications see Section 4.3) will be shown and discussed in integral form according to

$$\Delta_{1,2}(\alpha') = \frac{1}{N_{\text{tot}}} \int_0^{\alpha'} (N(\alpha)_1 - N(\alpha)_2) d\alpha. \quad (16)$$

Such an integral representation<sup>1</sup> has the advantage that consistent trends in the differences  $\delta$  over extended ranges of  $\alpha$  become clearly visible even if they are small and noisy. Values  $\alpha_{\text{ext}}$  at which  $\Delta$  is maximal (minimal) correspond to the onset of negative (positive) differences  $\delta$  after an extended range  $\alpha < \alpha_{\text{ext}}$  of positive (negative) differences  $\delta$ . Hence, an extremum in  $\Delta$  indicates that the differences  $\delta$  giving rise to it are at  $\alpha < \alpha_{\text{ext}}$ .

As an example, the dotted line in Figure 2 shows the differences  $\delta_{1,2}$  of two histograms. They are calculated for each  $\alpha$  bin separately and normalized with

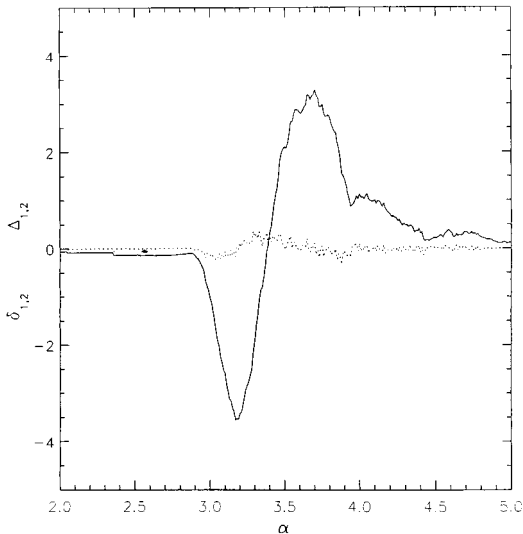


Fig. 2. Example of differential and integral representations of the differences between two  $N(\alpha)$  histograms. Dotted line: relative normalized differences  $\delta_{1,2}$  for each bin. Solid line: relative normalized integral differences  $\Delta_{1,2}$  (same as dotted line in Figure 4).

<sup>1</sup>As always, integrals are numerically evaluated by a sum of finitely many terms, here given by the values of  $N(\alpha)$  within bins of  $\Delta\alpha=0.01$ .

respect to the total number  $N_{\text{tot}}$  of points. The solid line in Figure 2 shows the corresponding integral plot of  $\Delta_{1,2}$ , again as relative deviations. For  $\alpha < \alpha_{\text{ext}} = 3.18$ , the differences  $\delta_{1,2}$  are consistently negative. This trend changes at  $\alpha_{\text{ext}} = 3.18$ , where  $\Delta_{1,2}$  is minimal and the differences  $\delta_{1,2}$  become positive. The relative deviation at  $\alpha_{\text{ext}} = 3.18$  is negative and amounts to  $\Delta_{1,2} \approx 3.56\%$ .

In order to obtain reasonable error estimates for the analysis, the fluctuations of such histograms for 100 different realizations of calibration data were considered. Subtracting each of the 100 individual  $N(\alpha)$  histograms from a mean  $N(\alpha)$  histogram, a mean fluctuation  $\langle \Delta_{\text{cal}} \rangle$  was determined as a function of  $\alpha$  (see Figure 3). The applied procedure, in detail described by Atmanspacher *et al.* (1999), is basically heuristic; further work to back it up formally is in progress. Insofar as the calibration data can be regarded as surrogate data (Theiler *et al.*, 1992), this mean fluctuation represents a proper error estimate for the histograms.

Values of  $\langle \Delta_{\text{cal}} \rangle$  that differ from zero quantify how much the density of an individual set of calibration data fluctuates around the density of an average distribution of calibration data with  $N_{\text{tot}} = 10,000$  on purely statistical grounds (given that the overall density is constant). Deviations in the left wing of  $N(\alpha)$  refer to “overdense” regions in the embedding space. They indicate that local correlations in an individual set of calibration data deviate from those of an average distribution of calibration data, *i.e.*, are more or less homogeneous than that average distribution (with a finite number of points). “Underdense” regions such as voids (characterized by “anti”- correlations) correspond to the right wing of  $N(\alpha)$  where errors typically are much larger and prevent any significant detection (Atmanspacher, Scheingraber and Wiedenmann, 1989).

In another publication (Atmanspacher *et al.*, 1999), other sets of surrogate

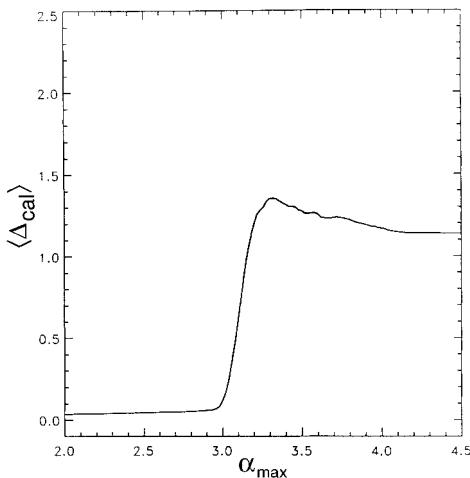


Fig. 3. Mean values (solid line) and standard deviations (shaded area) of  $\Delta(\alpha_{\text{max}})$  for the maxima of  $|\Delta_{\text{cal}}|$  as a function of  $\alpha_{\text{max}}$ .

data such as fitted Gaussian distributions and various kinds of Monte Carlo permuted data were studied in addition. It turned out that fluctuations as obtained from the calibration data are both most conservative and most realistic for an error estimate with respect to our present purposes. The detailed procedures and arguments can be found in Atmanspacher *et al.* (1999).

### 4.3 Some First Results

The empirical material analyzed was taken from a series of experiments carried out at the Institut für Grenzgebiete der Psychologie und Psychohygiene (IGPP) at Freiburg. The purpose of the IGPP study is a replication of the results obtained by PEAR as briefly summarized in Section 4.1. Only those agents were selected for the analysis who had finished 10 sessions within the IGPP replication study by the end of September 1997. Due to the experimental protocol, the corresponding amount of data is 10,000 per mode of intention and per agent. Therefore, individual agents were coded by numbers (1, ..., 16), and modes of intention were randomly coded by numbers (1, 2, 3) for each agent separately before the data were released for analysis. Hence the analysis itself amounts to nothing else than an analysis of deviations from randomness. In particular, it does not make use of any information concerning correlations with psychological observables.

Time series provided by sequences of 10,000 data points per intentional mode for each agent have been analyzed, regardless of any other possible discriminations. This is to say that we disregarded any information other than the distinction between different but unknown (not yet decoded) modes of intention. In other words: we assume that each sequence of 10,000 data points represents a statistical ensemble. The reason is that pilot studies showed that possible deviations from randomness have to be expected so small that a sensible scaling index analysis requires data series of at least 10,000 points to be analyzed in at least four dimensions,  $d = 4$ . (Other parameters are as given in Section 4.2.) More detailed studies (with shorter time series) may be possible if agents can be identified for which major deviations from randomness are observed.

The first step of the analysis was the determination of the relative integral differences between the  $N(\alpha)$  histogram for a suitable representative for a random sequence and the three  $N(\alpha)$  histograms corresponding to the three modes of intention for each agent. Selecting the mean histogram over all calibration data (Section 4.2) as such a suitable representative,

$$\Delta_{\text{cal,int}} = \frac{1}{N_{\text{tot}}} \int_0^{\alpha'} (\langle N(\alpha)_{\text{cal}} \rangle - N(\alpha)_{\text{int}}) d\alpha \quad (17)$$

was calculated for each agent and mode of intention. The solid line in Figure 2 represents  $\Delta_{\text{cal,int}}$  as a function of  $\alpha$  for intentional mode #2 of agent #16. There is a prominent negative peak of 3.56% at  $\alpha = 3.18$ , where the corresponding error is 1.1 (see Figure 3). This means that the deviation from

randomness in this example is significant with  $3.2\sigma$  (corresponding to  $p \approx 0.0017$ ). It represents the most pronounced effect resulting from an analysis of the extrema of  $\Delta_{\text{cal,int}}$ .

The significances of differences  $\Delta$  might be underestimated if one considers only the extrema of  $\Delta$ . This is due to the fact that the errors in the critical range  $2.9 < \alpha < 3.3$  depend strongly on  $\alpha$ . As a consequence, deviations smaller than their extrema may be more significant than those at the extrema, particularly if they are located at small enough values of  $\alpha$ . For this reason, it is interesting to check the dependence of significance of deviations on  $\alpha$  in addition to the deviations themselves. For instance, the significance of deviations for agent #16/intention #2 turns out to be highest at  $\alpha = 2.98$  where an overwhelming  $9.52\sigma$  is obtained.

Significances of deviations from randomness and additional features due to other agents and modes of intention are summarized in Figure 6 and Table 2 of Atmanspacher *et al.* (1999). It is remarkable that those data points contributing to significant deviations from randomness refer almost exclusively to states or transitions between states, respectively, located within a small stripe ( $\approx \pm 5$ ) around the mean  $\langle x \rangle = 100$ . This implies that major deviations are not caused by (transitions between) states far away from  $\langle x \rangle$ . Lucadou (1986) reported a similar observation with respect to his preferred observable “pragmatic information.” The relationship between this observable and dynamical randomness remains to be clarified.

Due to the fact that the deviations for agent #16 are so prominent, it has been checked whether they can also be observed with 3-dimensional rather than 4-dimensional embedding. Reducing the embedding dimension to three makes it possible to analyze the 10 sessions (comprising 10,000 data points altogether) individually. The characteristic features indicating non-random contributions remain pronounced for all 10 sessions with 1000 data points each; quantitative significances have not yet been determined. It is remarkable that the characteristic features are homogeneously distributed over the sessions. This underlines the option to further analyze the empirical material concerning agent #16.

Since the analysis as performed in this study is sensitive to deviations from randomness in the transition probabilities as well as state probabilities, it is desirable to distinguish between these different types of non-randomness in the experimental data. If the deviations are due to temporal correlations, they should vanish (or at least decrease) for a Monte Carlo randomization of the sequence of states. This can be tested by generating random permutations of the time series taken under agent intention and subtracting the resulting  $N(\alpha)$  histogram from the mean histogram of the calibration data. It turned out that all significant deviations drop well below  $2\sigma$  if the corresponding sequences are randomized.

The hypothesis that we are dealing with deviations from randomness in the transition probabilities rather than randomness with respect to states can be

further backed up by a simulation of small temporal correlations within an otherwise random time series. As an example, one can replace a small proportion, say 60 randomly selected sets of three successive data points (“triplets”) in a random series of calibration data with  $N_{\text{tot}} = 10,000$  by 60 ordered triplets of the form  $\{91, 93, 95\}$ . Analyzing the modified time series according to the procedure described above leads to deviations  $\Delta$  from the mean calibration distribution which are plotted as a solid line in Figure 4. The dotted line in the same figure reproduces (from Figure 2) the deviations obtained for agent #16 intention #2.

### 5. Concluding Remarks

The applied analysis was basically used as a non-parametric procedure to check the hypothesis of randomness in the data. There are strong indications that this hypothesis is rejected for some agents. Therefore, our results do strongly encourage further investigations of deviations from randomness in physically random devices and their relationship to the intention of human agents with appropriate techniques. In particular, it seems worthwhile to focus on the *dynamical* aspects of such deviations in addition to more straightforward analyses of state probabilities. There are some immediate options for future lines of research.

1. As soon as the identification of agents and modes of intention in the IGPP study is revealed, it will be interesting to see in which way

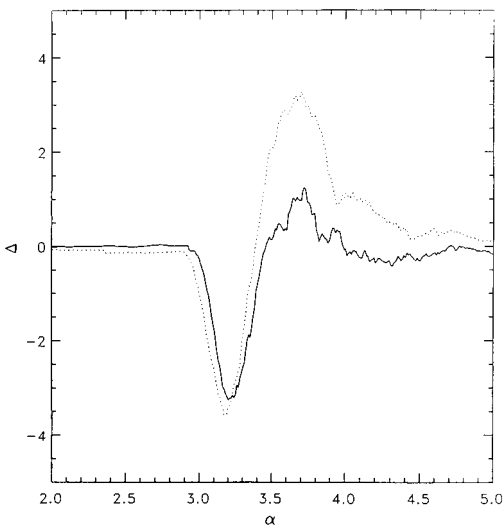


Fig. 4. Solid line: relative normalized integral differences  $\Delta$  between the  $N(\alpha)$  histograms of a distribution with 60 ordered triplets and a mean random calibration distribution. Dotted line: relative normalized integral differences  $\Delta$  between the  $N(\alpha)$  histograms of the distribution corresponding to agent #16/intention #2 and a mean random calibration distribution (same as solid line in Figure 2).

intentional modes (and/or other psychological observables) correlate with deviations from dynamical randomness. Moreover, it has to be investigated whether those agents (*e.g.*, #16) generating such deviations are able to reproduce them.

2. Experimental results from more agents than studied so far are to be analyzed. In addition to material that can be provided by IGPP and a similar replication study at the University of Giessen, there is a tremendously rich data pool at PEAR. These data will be systematically surveyed in the near future.
3. The scaling index analysis allows us to identify those data points contributing to the observed deviations from randomness. Since they are typically located in a small stripe around the mean  $\langle x \rangle = 100$ , a search for patterns in those points is considerably facilitated. It is not yet clear whether such patterns are of the type giving rise to the solid line in Figure 4. The relationship between significantly non-random features in the scaling indices and the underlying stochastic process is both highly non-trivial and non-unique. Further work is necessary to explore this issue in more detail.

Finally, it should be emphasized that the results presented so far are *not* to be understood in terms of a “proof” for the “reality” of yet unknown relationships between physical and mental systems. Statistical analyses can indicate evidence for something but never “prove” its “reality.” Furthermore, we do not think that adding more results of the same kind to the existing material would change the situation with respect to its broader acceptance. Such results will not be accepted in the corpus of serious scientific knowledge unless plausible concepts concerning the context under which they occur can be presented.

For these reasons there is no particular value in an analysis of the overall evidence for deviations from dynamical randomness for the full sample of 16 agents with three modes of intention each. Our research strategy focuses on a step-by-step procedure oriented toward understanding the origin of and the boundary conditions for those deviations for which the applied analysis indicates evidence. If at all, this can be done most effectively with those agents who seem to be capable of generating them.

### Acknowledgments

We are grateful to Werner Ehm, Jürgen Kurths, and Gerda Wiedenmann for helpful comments.

### References

- Atmanspacher, H., Bösch, H., Boller, E., Scheingraber, H., & Nelson, R. D. (1999). Deviations from physical randomness due to human agent intention? *Chaos, Solitons, & Fractals*, *10*, 935–952.
- Atmanspacher, H., R ath, C., & Wiedenmann, G. (1997). Statistics and meta-statistics in the concept of complexity. *Physica A*, *234*, 819–829.

- Atmanspacher, H., Scheingraber, H., & Wiedenmann, G. (1989). Determination of  $f(\alpha)$  for a limited random point set. *Physical Review A*, *40*, 3954–3963.
- Atmanspacher, H., Wiedenmann, G., & Amann, A. (1995). Descartes revisited: the endo/exodistinction and its relevance for the study of complex systems. *Complexity*, *1*, 3, 15–21.
- Bradish, G. J. (1993). PEAR portable REG prescription for operation. Technical Note of June 15, 1993.
- Deco, G., Schittenkopf, C., & Schürmann, B. (1997). Dynamical analysis of time series by statistical tests. *International Journal of Bifurcations and Chaos*, *7*, 2629–2652.
- Delanoy, D. L. (1996). Experimental evidence suggestive of anomalous consciousness interactions. *Biomedical and Life Physics*, ed. by N. Ghista. Braunschweig: Vieweg, 397–410.
- Doob, J. L. (1953). *Stochastic processes*. New York: Wiley.
- Feller, W. (1950). *An introduction to probability theory and its applications, Vol. 1*. New York: Wiley.
- Gaspard, P., & Wang, X. J. (1993). Noise, chaos, and  $(\epsilon, \tau)$ -entropy per unit time. *Physical Review A*, *235*, 291–343.
- Grassberger, P., Badii, R., & Politi, A. (1988). Scaling laws for invariant measures on hyperbolic and nonhyperbolic attractors. *Journal of Statistical Physics*, *51*, 135–178.
- Halsey, T. C., Jensen, M. H., Kadanoff, L. P., Procaccia, I., & Shraiman, B. I. (1986). Fractal measures and their singularities: the characterization of strange sets. *Physical Review A*, *33*, 1141–1151.
- Jahn, R. G., Dunne, B. J., Nelson, R. D., Dobyns, Y. H., & Bradish, G. J. (1997). Correlations of random binary sequences with pre-stated operator intention: a review of a 12-year program. *Journal of Scientific Exploration*, *11*, 345–367.
- Kantz, H., Kurths, J., & Mayer-Kress, G., eds. (1998). *Nonlinear analysis of physiological data*. Berlin: Springer.
- Kantz, H., & Schreiber, T. (1997). *Nonlinear time series analysis*. Cambridge: Cambridge University Press.
- Kurths, J., Voss, A., Saperin, P., Witt, A., Kleiner, H. J., & Wessel, N. (1995). Quantitative analysis of heart rate variability. *CHAOS*, *5*, 88–94.
- von Lucadou, W. (1986). *Experimentelle Untersuchungen zur Beeinflussbarkeit von stochastischen quantenphysikalischen Systemen durch den Beobachter*. Frankfurt: Herchen, p. 225.
- Mandelbrot, B.B. (1974). Intermittent turbulence in self-similar cascades: divergence of high moments and dimension of the carrier. *Journal of Fluid Mechanics*, *62*, 331–358.
- Morfill, G. E., Demmel, V., & Schmidt, G. (1994). Der plötzliche Herztod. Neue Erkenntnisse durch die Anwendung komplexer Diagnoseverfahren. *Bioscope*, *2/94*, 11–19.
- Nelson, R. D., Bradish, G. J., & Dobyns, Y. H. (1989). Random event generator qualification, calibration, and analysis. Technical Note PEAR 89001, April 1989.
- Packard, N. H., Crutchfield, J. P., Farmer, J. D., & Shaw, R. S. (1980). Geometry from a time series. *Physical Review Letters*, *45*, 712–716.
- Paladin, G., & Vulpiani, A. (1987). Anomalous scaling laws in multifractal objects. *Physics Reports*, *156*, 147–225.
- Priestley, M. B. (1988). *Non-linear and non-stationary time series analysis*. London: Academic Press.
- Räth, C., & Morfill, G. (1997). Texture detection and texture discrimination with anisotropic scaling indices. *Journal of the Optical Society of America A*, *14*, 3208–3215.
- Rosenblum, M. G., Pikovsky, A. S., & Kurths, J. (1996). Phase synchronization of chaotic oscillators. *Physical Review Letters*, *76*, 1804–1807.
- Schmidt, H. (1970). A PK test with electronic equipment. *Journal of Parapsychology*, *34*, 175–181.
- Schreiber, T. (1999). Interdisciplinary application of nonlinear time series methods. *Physics Reports*, *308*, 1–64.
- Siffing, R. (1996). *Phasenraumbetrachtungen bei synchronen Zeitreihen*. Diploma thesis, Universität München.
- Theiler, J., Eubank, S., Longtin, A., Galdrikian, B., & Farmer, J. D. (1992). Testing for nonlinearity in time series: the method of surrogate data. *Physica D*, *58*, 77–94.
- Tong, H. (1990). *Non-linear time series analysis*. Oxford: Oxford University Press.
- Utts, J. (1991). Replication and meta-analysis in parapsychology. *Statistical Science*, *6*, 363–403.
- Wackerbauer, R., Witt, A., Atmanspacher, H., Kurths, J., & Scheingraber, H. (1994). A comparative classification of complexity measures. *Chaos, Solitons, & Fractals*, *4*, 133–173.

- Wiedenmann, G., Scheingraber, H., & Voges, W. (1997). Source detection with the scaling index method. In *Data Analysis in Astronomy 5*, eds. di Gesu, V. *et al.* Singapore: World Scientific, 203–211.
- Young, K., & Crutchfield, J. P. (1994). Fluctuation spectroscopy. *Chaos, Solitons, & Fractals*, 4, 5–39.